

Guaranteed Performance Nonlinear Observer for Simultaneous Localization and Mapping

Hashim A. Hashim

Abstract—A geometric nonlinear observer algorithm for Simultaneous Localization and Mapping (SLAM) developed on the Lie group of $\text{SLAM}_n(3)$ is proposed. The presented novel solution estimates the vehicle's pose (*i.e.* attitude and position) with respect to landmarks simultaneously positioning the reference features in the global frame. The proposed estimator on manifold is characterized by predefined measures of transient and steady-state performance. Dynamically reducing boundaries guide the error function of the system to reduce asymptotically to the origin from its starting position within a large given set. The proposed observer has the ability to use the available velocity and feature measurements directly. Also, it compensates for unknown constant bias attached to velocity measurements. Unit-quaternion of the proposed observer is presented. Numerical results reveal effectiveness of the proposed observer.

Index Terms—Nonlinear filter algorithm, Simultaneous Localization and Mapping, asymptotic stability, systematic convergence, pose, attitude, position, landmark, adaptive estimate, SLAM, $\text{SE}(3)$, $\text{SO}(3)$.

I. INTRODUCTION

NAVIGATION solutions, in the age of autonomous vehicles, suitable for both partially and entirely unknown environments are an absolute necessity. Autonomous navigation systems are an integral part of a variety of applications including household autonomous devices, mine exploration, location of missing terrestrial, underwater vehicles and others. The nature of these applications limits the usefulness of absolute positioning systems, such as global positioning systems (GPS) which require visibility of at least four satellites. In the absence of GPS, other techniques are used. If pose of a robot or vehicle is known, while the map of its surroundings is unknown, the problem is referred to as a mapping problem [1]. On the contrary, if the map of the environment is known, while the pose is unknown, the problem is described as pose estimation [2–5]. Simultaneous Localization and Mapping (SLAM) combines mapping and pose estimation problems and requires the autonomous system to simultaneously build a map of the environment and track its own pose (*i.e.* attitude and position) within that environment. SLAM problem can be solved using a set of measurements available at the body-fixed frame of the vehicle.

Over the last few decades, Gaussian filters played a significant role in solving the SLAM problem by positioning both the vehicle and its surrounding features. Commonly used

algorithms include FastSLAM [6], incremental SLAM [7], particle filter [8], and invariant EKF [9]. The SLAM algorithms proposed in [6–10] are based on probabilistic approach. Over a decade ago, graphical maximum likelihood algorithms have been widely explored [11,12]. Aside from Gaussian filtering methods, the true SLAM problem is a dual estimation problem which is highly nonlinear in nature, and evolves directly on the Lie group of $\text{SLAM}_n(3)$ which will be defined in the next Section. For instance, the pose dynamics are modeled on the Lie group of the special Euclidean group $\text{SE}(3)$. Over the last ten years, several nonlinear observers developed directly on $\text{SE}(3)$ have been proposed, for instance [2,4]. As a result, manifolds and the inheritance of the Lie group of $\text{SE}(3)$ in the SLAM problem was studied [13,14]. A two stage observer for SLAM has been presented in [15] where the first stage consists of a nonlinear pose observer, while the second stage is comprised of a Kalman filter used for feature estimation. Nevertheless, the above approach did not capture the true nonlinearity of the SLAM problem. Although the nonlinear observers proposed in [16,17] mimic the nonlinear structure of the true SLAM problem, they lack measures of the error convergence for the transient and steady-state performance.

This work introduces a novel nonlinear observer evolved directly on the Lie group of $\text{SLAM}_n(3)$ using velocity and feature measurements. In view of practical implementation and similar to [17], the velocity measurements are assumed to be corrupted with unknown bias. With the aim of achieving systematic convergence of the SLAM error function, the error is constrained to initiate among a predefined known large set and reduce systematically and smoothly obeying predefined dynamically reducing boundaries and to settle within a known small set, unlike to [17]. Prescribed performance function (PPF) captures the concept of systematic convergence [18]. PPF forces the error to be constrained by introducing a new form of unconstrained error, termed transformed error. The nonlinear observer is designed such that the SLAM error function as well as the transformed error can be proven to be globally asymptotically stable.

The Introduction section is followed by five sections, where Section II overviews mathematical notation, Lie group of $\text{SE}(3)$, and $\text{SLAM}_n(3)$. Section III introduces the SLAM problem along with available measurements. Section IV reformulates the SLAM problem to satisfy PPF and presents a nonlinear observer design on $\text{SLAM}_n(3)$ with systematic convergence. Section V includes simulation results. Finally, Section VI concludes the work.

This work was supported in part by Thompson Rivers University Internal research fund, RGS-2020/21 IRF, # 102315.

Corresponding author, H. A. Hashim is with the Department of Engineering and Applied Science, Thompson Rivers University, Kamloops, British Columbia, Canada, V2C-0C8, e-mail: hhashim@tru.ca.

II. PRELIMINARIES AND MATH NOTATION

Consider a vehicle traveling in three dimensional (3D) space. The vehicle fixed body-frame is described by $\{\mathcal{B}\}$ and the absolute fixed inertial-frame is described by $\{\mathcal{I}\}$. The set of real numbers, nonnegative real numbers, and real n -by- m space, are defined by \mathbb{R} , \mathbb{R}_+ , and $\mathbb{R}^{n \times m}$, respectively. \mathbf{I}_n refers to n -dimensional identity matrix, $\mathbf{0}_n$ describes a zero column vector. For $x \in \mathbb{R}^n$ the Euclidean norm is $\|x\| = \sqrt{x^\top x}$. Vehicle attitude is described by $R \in \mathbb{SO}(3)$ where $\mathbb{SO}(3)$ denotes Special Orthogonal Group such that $\mathbb{SO}(3) = \{R \in \mathbb{R}^{3 \times 3} \mid RR^\top = \mathbf{I}_3, \det(R) = +1\}$ with $\det(\cdot)$ representing a determinant, visit [19,20]. $\mathbf{T} \in \mathbb{R}^{4 \times 4}$ describes the vehicle's pose in 3D space expressed as

$$\mathbf{T} = \begin{bmatrix} R & P \\ \mathbf{0}_3^\top & 1 \end{bmatrix} \in \mathbb{SE}(3) \quad (1)$$

where $P \in \mathbb{R}^3$ refers to the vehicle's position, $R \in \mathbb{SO}(3)$ defines vehicle's attitude, and $\mathbb{SE}(3)$ refers to Special Euclidean Group described by $\mathbb{SE}(3) = \{\mathbf{T} \in \mathbb{R}^{4 \times 4} \mid R \in \mathbb{SO}(3), P \in \mathbb{R}^3\}$, visit [2]. $\mathfrak{so}(3)$ is the Lie-algebra of $\mathbb{SO}(3)$ described by $\mathfrak{so}(3) = \{[y]_\times \in \mathbb{R}^{3 \times 3} \mid [y]_\times^\top = -[y]_\times, y \in \mathbb{R}^3\}$ with $[y]_\times$ denoting a skew symmetric matrix

$$[y]_\times = \begin{bmatrix} 0 & -y_3 & y_2 \\ y_3 & 0 & -y_1 \\ -y_2 & y_1 & 0 \end{bmatrix} \in \mathfrak{so}(3), \quad y = \begin{bmatrix} y_1 \\ y_2 \\ y_3 \end{bmatrix}$$

$\mathfrak{se}(3)$ is the Lie-algebra of $\mathbb{SE}(3)$ with

$$\mathfrak{se}(3) = \left\{ [U]_\wedge \in \mathbb{R}^{4 \times 4} \mid \exists \Omega, V \in \mathbb{R}^3 : [U]_\wedge = \begin{bmatrix} [\Omega]_\times & V \\ \mathbf{0}_3^\top & 0 \end{bmatrix} \right\}$$

where $U = [\Omega^\top, V^\top] \in \mathbb{R}^6$. Consider that $\mathbf{T} \in \mathbb{SE}(3)$ as defined in (1) and $U \in \mathbb{R}^6$. Define the adjoint map $\text{Ad}_{\mathbf{T}} : \mathbb{SE}(3) \times \mathfrak{se}(3) \rightarrow \mathfrak{se}(3)$ and the augmented adjoint map $\overline{\text{Ad}}_{\mathbf{T}} : \mathbb{SE}(3) \rightarrow \mathbb{R}^{6 \times 6}$ as below

$$\begin{cases} \text{Ad}_{\mathbf{T}}([U]_\wedge) &= \mathbf{T} [U]_\wedge \mathbf{T}^{-1} \in \mathfrak{se}(3) \\ \overline{\text{Ad}}_{\mathbf{T}} &= \begin{bmatrix} R & \mathbf{0}_{3 \times 3} \\ [P]_\times R & R \end{bmatrix} \in \mathbb{R}^{6 \times 6} \end{cases} \quad (2)$$

In view of (2), one finds

$$\text{Ad}_{\mathbf{T}}([U]_\wedge) = [\overline{\text{Ad}}_{\mathbf{T}} U]_\wedge, \quad \mathbf{T} \in \mathbb{SE}(3), U \in \mathbb{R}^6 \quad (3)$$

Define the sub-manifolds $\mathring{\mathcal{M}}$ and $\overline{\mathcal{M}}$ of \mathbb{R}^4 as

$$\begin{aligned} \mathring{\mathcal{M}} &= \left\{ \mathring{y} = \begin{bmatrix} y^\top & 0 \end{bmatrix}^\top \in \mathbb{R}^4 \mid y \in \mathbb{R}^3 \right\} \\ \overline{\mathcal{M}} &= \left\{ \overline{y} = \begin{bmatrix} y^\top & 1 \end{bmatrix}^\top \in \mathbb{R}^4 \mid y \in \mathbb{R}^3 \right\} \end{aligned}$$

Let the Lie group of $\mathbb{SLAM}_n(3) = \mathbb{SE}(3) \times \overline{\mathcal{M}}^n$ be

$$\mathbb{SLAM}_n(3) = \left\{ X = (\mathbf{T}, \overline{\mathbf{p}}) \mid \mathbf{T} \in \mathbb{SE}(3), \overline{\mathbf{p}} \in \overline{\mathcal{M}}^n \right\} \quad (4)$$

where $\overline{\mathbf{p}} = [\overline{\mathbf{p}}_1, \overline{\mathbf{p}}_2, \dots, \overline{\mathbf{p}}_n] \in \overline{\mathcal{M}}^n$ and $\overline{\mathcal{M}}^n = \overline{\mathcal{M}} \times \overline{\mathcal{M}} \times \dots \times \overline{\mathcal{M}}$. Describe the tangent space at the identity element of $X = (\mathbf{T}, \overline{\mathbf{p}}) \in \mathbb{SLAM}_n(3)$ as $\mathfrak{slam}_n(3) = \mathfrak{se}(3) \times \mathring{\mathcal{M}}^n$

$$\mathfrak{slam}_n(3) = \left\{ \mathcal{Y} = ([U]_\wedge, \mathring{v}) \mid [U]_\wedge \in \mathfrak{se}(3), \mathring{v} \in \mathring{\mathcal{M}}^n \right\} \quad (5)$$

where $\mathring{v} = [\mathring{v}_1, \mathring{v}_2, \dots, \mathring{v}_n] \in \mathring{\mathcal{M}}^n$, $\mathring{\mathcal{M}}^n = \mathring{\mathcal{M}} \times \mathring{\mathcal{M}} \times \dots \times \mathring{\mathcal{M}}$, and $\mathring{v}_i = [\mathring{v}_i^\top, 0]^\top \in \mathring{\mathcal{M}}$. Also, $\overline{\mathbf{p}}_i = [\mathbf{p}_i^\top, 1]^\top \in \overline{\mathcal{M}}$.

III. PROBLEM FORMULATION

Consider a vehicle moving in 3D space within a map that has n features. SLAM problem is the process of estimating vehicle pose $\mathbf{T} \in \mathbb{SE}(3)$, and at the same time estimating n features within the environment $\overline{\mathbf{p}} = [\overline{\mathbf{p}}_1, \overline{\mathbf{p}}_2, \dots, \overline{\mathbf{p}}_n] \in \overline{\mathcal{M}}^n$. Fig. 1 provides a conceptual illustration of the SLAM estimation problem.

Consider $R \in \mathbb{SO}(3)$ and $P \in \mathbb{R}^3$ to be vehicle's attitude (orientation) and position, respectively, and $\mathbf{p}_i \in \mathbb{R}^3$ to be the i th feature position in the map, where $R \in \{\mathcal{B}\}$, and $P, \mathbf{p}_i \in \{\mathcal{I}\}$ for all $i = 1, 2, \dots, n$. Let $X = (\mathbf{T}, \overline{\mathbf{p}}) \in \mathbb{SLAM}_n(3)$ be the true pose and features with $\mathbf{T} \in \mathbb{SE}(3)$ and $\overline{\mathbf{p}} \in \overline{\mathcal{M}}^n$. Let $\mathcal{Y} = ([U]_\wedge, \mathring{v}) \in \mathfrak{slam}_n(3)$ be the true group velocity where $\mathring{v} = [\mathring{v}_1, \mathring{v}_2, \dots, \mathring{v}_n] \in \mathring{\mathcal{M}}^n$ and $U, \mathring{v} \in \{\mathcal{B}\}$. The true motion dynamics of SLAM are as follows:

$$\begin{cases} \dot{\mathbf{T}} &= \mathbf{T} [U]_\wedge \\ \dot{\mathbf{p}}_i &= R \mathbf{v}_i, \quad \forall i = 1, 2, \dots, n \end{cases} \quad (6)$$

where $U = [\Omega^\top, V^\top]^\top$, $\Omega \in \mathbb{R}^3$ is the true angular velocity, $V \in \mathbb{R}^3$ is the true translational velocity, while $\mathbf{v}_i \in \mathbb{R}^3$ describes the i th linear velocity of \mathbf{p}_i . X is unknown and can be obtained with the aid of 1) $\mathcal{Y}_m = ([U_m]_\wedge, \mathring{v}_m) \in \mathfrak{slam}_n(3)$ which represents velocity measurements and 2) $\overline{y}_i \in \overline{\mathcal{M}}$ which is the i th feature measurement for all $\mathcal{Y}_m, \overline{y}_i \in \{\mathcal{B}\}$. Since features are fixed to $\{\mathcal{I}\}$, $\dot{\mathbf{p}}_i = \mathbf{0}_3$ and consequently $\mathbf{v}_i = \mathbf{0}_3$. The measurement of the group velocity $U_m = [\Omega_m^\top, V_m^\top]^\top$ is

$$U_m = U + b_U + n_U \in \mathbb{R}^6 \quad (7)$$

where $b_U = [b_\Omega^\top, b_V^\top]^\top$ is unknown constant bias and n_U denotes random noise. The i th feature measurement in the body-frame is described by

$$\overline{y}_i = \mathbf{T}^{-1} \overline{\mathbf{p}}_i + \mathring{b}_i^y + \mathring{n}_i^y \in \overline{\mathcal{M}}, \quad \forall i = 1, 2, \dots, n \quad (8)$$

where $\mathring{b}_i^y \in \mathring{\mathcal{M}}$ and $\mathring{n}_i^y \in \mathring{\mathcal{M}}$ represent unknown constant bias and random noise, respectively. Also, $\overline{\mathbf{p}}_i = [\mathbf{p}_i^\top, 1]^\top \in \overline{\mathcal{M}}$ denotes the i th feature. In our analysis, n_U , b_i^y , and n_i^y are zeros.

Assumption 1. Three or more features available for measurement that define a plane with $\overline{y} = [\overline{y}_1, \overline{y}_2, \dots, \overline{y}_n] \in \overline{\mathcal{M}}^n$.

Define the estimate of pose as

$$\hat{\mathbf{T}} = \begin{bmatrix} \hat{R} & \hat{P} \\ \mathbf{0}_3^\top & 1 \end{bmatrix} \in \mathbb{SE}(3)$$

where \hat{R} and \hat{P} represent estimates of the true orientation and position, respectively. Define $\hat{\mathbf{p}}_i$ as the estimate of the true i th feature \mathbf{p}_i . Consider the error between \mathbf{T} and $\hat{\mathbf{T}}$ as

$$\begin{aligned} \tilde{\mathbf{T}} = \hat{\mathbf{T}} \mathbf{T}^{-1} &= \begin{bmatrix} \hat{R} & \hat{P} \\ \mathbf{0}_3^\top & 1 \end{bmatrix} \begin{bmatrix} R^\top & -R^\top P \\ \mathbf{0}_3^\top & 1 \end{bmatrix} \\ &= \begin{bmatrix} \tilde{R} & \tilde{P} \\ \mathbf{0}_3^\top & 1 \end{bmatrix} \end{aligned} \quad (9)$$

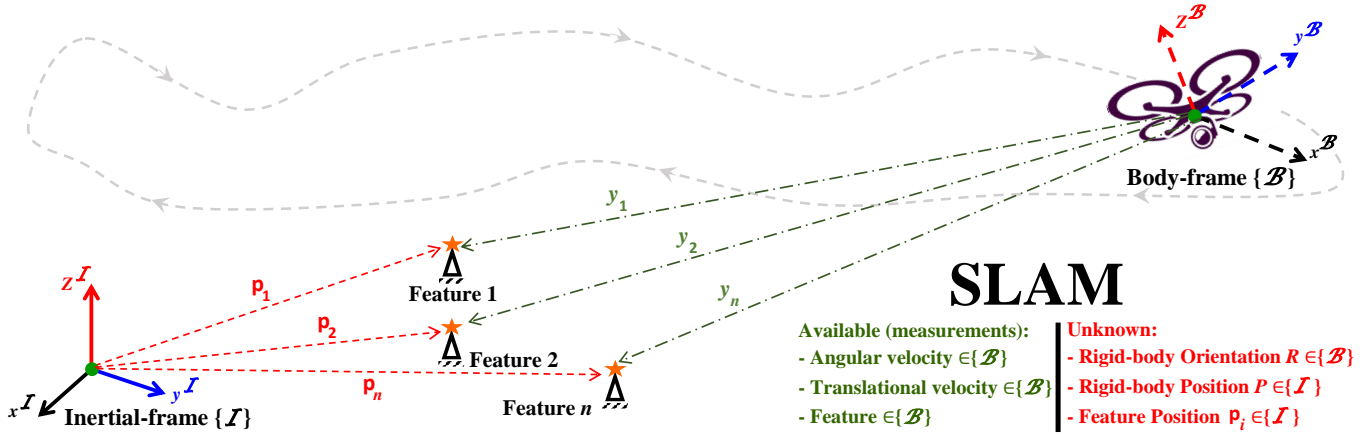


Fig. 1. SLAM estimation problem.

with $\tilde{R} = \hat{R}R^\top$ and $\tilde{P} = \hat{P} - \tilde{R}P$ describing error in orientation and position, respectively. Define the error between \hat{p}_i and p_i as

$$\hat{e}_i = \tilde{p}_i - \tilde{T}\tilde{p}_i \quad (10)$$

where $\hat{e}_i = [e_i^\top, 0]^\top \in \hat{\mathcal{M}}$ and $\tilde{p}_i = [\hat{p}_i^\top, 1]^\top \in \tilde{\mathcal{M}}$. In the light of \tilde{T} , definition in (9), and (8),

$$\begin{aligned} \hat{e}_i &= \tilde{p}_i - \hat{T}\tilde{T}^{-1}\tilde{p}_i \\ &= \tilde{p}_i - \hat{T}\tilde{y}_i \end{aligned} \quad (11)$$

Accordingly, $\hat{e}_i = [(\tilde{p}_i - \tilde{P})^\top, 0]^\top$ where $\tilde{p}_i = \hat{p}_i - \tilde{R}p_i$ represents the i th error in feature estimation, and $\tilde{P} = \hat{P} - \tilde{R}P$ as expressed in (9). To achieve adaptive estimation, let $\hat{b}_U = [\hat{b}_\Omega^\top, \hat{b}_V^\top]^\top$ be the estimate of the unknown bias b_U and let the error between them be

$$\tilde{b}_U = b_U - \hat{b}_U \in \mathbb{R}^6 \quad (12)$$

with $\tilde{b}_U = [\tilde{b}_\Omega^\top, \tilde{b}_V^\top]^\top$. As mentioned previously, the true SLAM kinematics in (6) are nonlinear modeled on Lie group of $\text{SLAM}_n(3) = \text{SE}(3) \times \tilde{\mathcal{M}}^n$ such that $X = (T, \tilde{p}) \in \text{SLAM}_n(3)$. Also, the tangent space of X is $\mathfrak{slam}_n(3) = \mathfrak{se}(3) \times \mathcal{M}^n$ with $\mathcal{Y} = ([U]_\wedge, \hat{v}) \in \mathfrak{slam}_n(3)$. Therefore, the proposed observer design has to 1) consider the nonlinear nature of the true SLAM problem and 2) be modeled on Lie group of $\text{SLAM}_n(3)$. Therefore, the observer proposed in the next section is defined by $\hat{X} = (\hat{T}, \hat{\tilde{p}}) \in \text{SLAM}_n(3)$ mimics the structure of the true SLAM problem with its tangent space being $\hat{\mathcal{Y}} = ([\hat{U}]_\wedge, \hat{v}) \in \mathfrak{slam}_n(3)$.

IV. NONLINEAR OBSERVER DESIGN WITH GUARANTEED PERFORMANCE

This section reformulates the SLAM kinematics such that the error function is guided by prescribed measures of transient and steady-state performance. Next, nonlinear observer design characterized by systematic convergence and reliant on available measurements is proposed.

A. Guaranteed Performance

The key objective of this subsection is to force $e_i = [e_{i,1}, e_{i,2}, e_{i,3}]^\top$ described in (11) to obey dynamically reducing transient boundaries and settle down within the narrow bounds adjusted by the user. A positive and time decreasing prescribed performance function (PPF) $\xi_{i,k}(t)$ with the map of $\xi_{i,k} : \mathbb{R}_+ \rightarrow \mathbb{R}_+$ [18,19] is employed to guide $e_{i,k}$ to initiate within a given large set $\xi_i^0 = [\xi_{i,1}^0, \xi_{i,2}^0, \xi_{i,3}^0]^\top \in \mathbb{R}^3$ and decay exponentially in accordance with a known convergence factor $\ell_i = [\ell_{i,1}, \ell_{i,2}, \ell_{i,3}]^\top \in \mathbb{R}^3$ causing $e_{i,k}$ to stay within a given small set $\xi_i^\infty = [\xi_{i,1}^\infty, \xi_{i,2}^\infty, \xi_{i,3}^\infty]^\top \in \mathbb{R}^3$ such that

$$\xi_{i,k}(t) = (\xi_{i,k}^0 - \xi_{i,k}^\infty) \exp(-\ell_{i,k}t) + \xi_{i,k}^\infty \quad (13)$$

for all $i = 1, 2, \dots, n$ and $k = 1, 2, 3$. The objective is $e_{i,k} = e_{i,k}(t)$ follows predefined convergence properties of $\xi_{i,k} = \xi_{i,k}(t)$ given that one of the following expressions is met:

$$-\delta_{i,k}\xi_{i,k} < e_{i,k} < \xi_{i,k}, \text{ if } e_{i,k}(0) \geq 0 \quad (14)$$

$$-\xi_{i,k} < e_{i,k} < \delta_{i,k}\xi_{i,k}, \text{ if } e_{i,k}(0) < 0 \quad (15)$$

where $\delta_{i,k} \in [0, 1]$. Fig. 2 provides an ample demonstration of the desired systematic convergence.

Remark 1. [19] For known $e_{i,k}(0)$ and granted that either provision (14) and (15) is fulfilled, the maximum undershoot/overshoot is guaranteed to adhere $\pm\delta\xi_{i,k}$ and the steady-state error to follows $\pm\xi_{i,k}^\infty$ in accordance with Fig. 2.

Define the error $e_{i,k}$ as

$$e_{i,k} = \xi_{i,k}\mathcal{F}(E_{i,k}) \quad (16)$$

where $\xi_{i,k} \in \mathbb{R}$ is as in (13), $E_{i,k} \in \mathbb{R}$ denotes unconstrained or transformed error, and $\mathcal{F}(E_{i,k})$ describes a smooth function that adheres to Assumption 2:

Assumption 2. $\mathcal{F}(E_{i,k})$ is a smooth function with the following characteristics [18]:

- 1) Strictly increasing,
- 2) Constrained by

$$\begin{cases} -\delta_{i,k} < \mathcal{F}(E_{i,k}) < \delta_{i,k}, & \text{if } e_{i,k}(0) \geq 0 \\ -\bar{\delta}_{i,k} < \mathcal{F}(E_{i,k}) < \bar{\delta}_{i,k}, & \text{if } e_{i,k}(0) < 0 \end{cases}$$

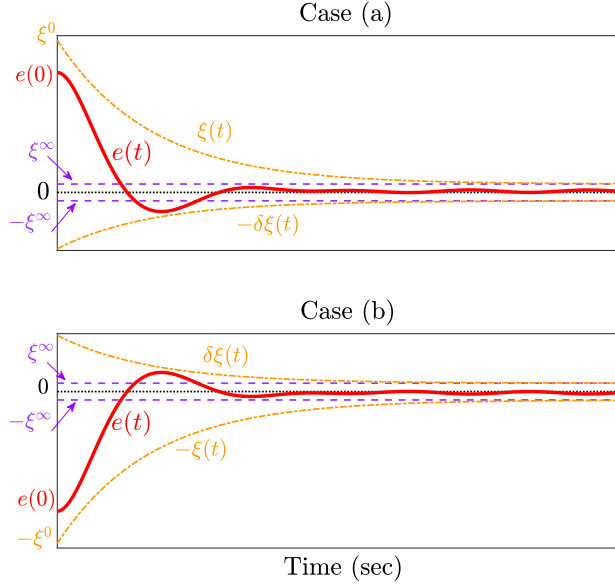


Fig. 2. $e_{i,k}$ based on systematic convergence (a) Eq. (14); (b) Eq. (15).

$$3) \quad \begin{aligned} & \text{with } \bar{\delta}_{i,k}, \underline{\delta}_{i,k} > 0 \text{ and } \underline{\delta}_{i,k} \leq \bar{\delta}_{i,k} \\ & \lim_{E_{i,k} \rightarrow -\infty} \mathcal{F}(E_{i,k}) = -\bar{\delta}_{i,k}, \text{ and } \lim_{E_{i,k} \rightarrow +\infty} \mathcal{F}(E_{i,k}) = \\ & \bar{\delta}_{i,k} \text{ if } e_{i,k}(0) \geq 0 \text{ or } \lim_{E_{i,k} \rightarrow -\infty} \mathcal{F}(E_{i,k}) = -\bar{\delta}_{i,k} \text{ and} \\ & \lim_{E_{i,k} \rightarrow +\infty} \mathcal{F}(E_{i,k}) = \underline{\delta}_{i,k} \text{ if } e_{i,k}(0) < 0. \end{aligned}$$

Define $\mathcal{F}(E_{i,k})$ as below

$$\mathcal{F}(E_{i,k}) = \frac{\bar{\delta}_{i,k} \exp(E_{i,k}) - \underline{\delta}_{i,k} \exp(-E_{i,k})}{\exp(E_{i,k}) + \exp(-E_{i,k})} \quad (17)$$

with $\bar{\delta}_{i,k} \geq \underline{\delta}_{i,k}$ if $e_{i,k}(0) \geq 0$ and $\underline{\delta}_{i,k} \geq \bar{\delta}_{i,k}$ if $e_{i,k}(0) < 0$.

The inverse transformation of (17) gives $E_{i,k} = E_{i,k}(e_{i,k}, \xi_{i,k})$

$$E_{i,k} = \mathcal{F}^{-1}(e_{i,k}/\xi_{i,k}) = \frac{1}{2} \ln \frac{\underline{\delta}_{i,k} + e_{i,k}/\xi_{i,k}}{\bar{\delta}_{i,k} - e_{i,k}/\xi_{i,k}} \quad (18)$$

where $\bar{\delta}_{i,k} \geq \underline{\delta}_{i,k}$ if $e_{i,k}(0) \geq 0$ and $\underline{\delta}_{i,k} \geq \bar{\delta}_{i,k}$ if $e_{i,k}(0) < 0$.
Let

$$\begin{aligned} \eta_{i,k} &= \frac{1}{2\xi_{i,k}} \frac{\partial \mathcal{F}^{-1}(e_{i,k}/\xi_{i,k})}{\partial (e_{i,k}/\xi_{i,k})} \\ &= \frac{1}{2\xi_{i,k}} \left(\frac{1}{\underline{\delta}_{i,k} + e_{i,k}/\xi_{i,k}} + \frac{1}{\bar{\delta}_{i,k} - e_{i,k}/\xi_{i,k}} \right) \end{aligned} \quad (19)$$

for all $i = 1, 2, \dots, n$ and $k = 1, 2, 3$. In the light of (19), define

$$\begin{cases} \mu_i &= \text{diag} \left(\frac{\xi_{i,1}}{\xi_{i,1}}, \frac{\xi_{i,2}}{\xi_{i,2}}, \frac{\xi_{i,3}}{\xi_{i,3}} \right), \quad \forall i = 1, 2, \dots, n \\ \Lambda_i &= \text{diag}(\eta_{i,1}, \eta_{i,2}, \eta_{i,3}) \end{cases} \quad (20)$$

To this end, the transformed error dynamics of $E_i = [E_{i,1}, E_{i,2}, E_{i,3}]^\top \in \mathbb{R}^3$ become equivalent to

$$\dot{E}_i = \Lambda_i (\dot{e}_i - \mu_i e_i), \quad \forall i = 1, 2, \dots, n \quad (21)$$

Note that μ_i is a vanishing element where $\mu_i \rightarrow 0$ as $t \rightarrow \infty$.

B. Nonlinear Observer Design

Consider the following nonlinear observer

$$\dot{\hat{T}} = \hat{T} \left[U_m - \hat{b}_U - W_U \right]_{\wedge} \quad (22)$$

$$\dot{\hat{p}}_i = -k_p (\Lambda_i + \Lambda_i^{-1}) E_i, \quad i = 1, 2, \dots, n \quad (23)$$

$$\dot{\hat{b}}_U = - \sum_{i=1}^n \frac{\Gamma}{\alpha_i} \overline{\text{Ad}}_{\hat{T}}^\top \left[\begin{array}{c} \hat{R}y_i + \hat{P} \\ \mathbf{I}_3 \end{array} \right]_{\times} \Lambda_i E_i \quad (24)$$

$$W_U = - \sum_{i=1}^n k_w \overline{\text{Ad}}_{\hat{T}}^{-1} \left[\begin{array}{c} \hat{R}y_i + \hat{P} \\ \mathbf{I}_3 \end{array} \right]_{\times} \Lambda_i E_i \quad (25)$$

where Λ_i and μ_i are defined in (20), k_p, k_w, Γ , and α_i are positive constants, $W_U = [W_U^\top, W_V^\top]^\top \in \mathbb{R}^6$ denotes a correction factor, $\hat{b}_U = [\hat{b}_U^\top, \hat{b}_V^\top]^\top \in \mathbb{R}^6$ is the estimate of b_U for all $W_\Omega, W_V, \hat{b}_\Omega, \hat{b}_V \in \mathbb{R}^3$. The unit-quaternion representation of the proposed observer is presented in Appendix.

Theorem 1. Consider the SLAM dynamics $\dot{X} = (\dot{T}, \dot{p})$ in (6) combined with velocity measurements ($U_m = U + b_U$) and output measurements ($\bar{y}_i = \mathbf{T}^{-1} \bar{p}_i$) for all $i = 1, 2, \dots, n$. Suppose that Assumption 1 holds and the observer design is as in (22), (23), (24), and (25). Select the design parameters k_p, k_w, Γ , and α_i as positive constants and $\bar{\delta}_{i,k} = \underline{\delta}_{i,k} \forall i = 1, 2, \dots, n$ and $k = 1, 2, 3$. Define the following set

$$\begin{aligned} \mathcal{S} &= \{(E_1, E_1, \dots, E_n) \in \mathbb{R}^3 \times \mathbb{R}^3 \times \dots \times \mathbb{R}^3 \\ & \quad | E_i = \mathbf{0}_3 \forall i = 1, 2, \dots, n\} \end{aligned} \quad (26)$$

Then, for $E_i(0) \in \mathcal{L}_\infty$, (1) the error (E_1, E_2, \dots, E_n) exponentially approaches \mathcal{S} , (2) the error (e_1, e_2, \dots, e_n) asymptotically approaches $(\mathbf{0}_3, \mathbf{0}_3, \dots, \mathbf{0}_3)$, (3) \hat{b}_U asymptotically converges to the origin, and (4) there exists a constant matrix $R_c \in \mathbb{S}\mathbb{O}(3)$ and a constant vector $P_c \in \mathbb{R}^3$ with $\lim_{t \rightarrow \infty} \hat{R} = R_c$ and $\lim_{t \rightarrow \infty} \hat{P} = P_c$.

Proof: Consider the pose error described in (9). The pose error dynamics are

$$\begin{aligned} \dot{\hat{T}} &= \dot{\hat{T}} \mathbf{T}^{-1} + \hat{T} \dot{\mathbf{T}}^{-1} \\ &= \hat{T} \left[U_m - \hat{b}_U - W_U \right]_{\wedge} \mathbf{T}^{-1} - \hat{T} \mathbf{T}^{-1} \dot{\mathbf{T}} \mathbf{T}^{-1} \\ &= \hat{T} \left[U + \tilde{b}_U - W_U \right]_{\wedge} \mathbf{T}^{-1} - \hat{T} [U]_{\wedge} \mathbf{T}^{-1} \\ &= \text{Ad}_{\hat{T}} \left(\left[\tilde{b}_U - W_U \right]_{\wedge} \right) \tilde{\mathbf{T}} \end{aligned} \quad (27)$$

Note that $\dot{\mathbf{T}}^{-1} = -\mathbf{T}^{-1} \dot{\mathbf{T}} \mathbf{T}^{-1}$. As such, the dynamics of \hat{e}_i in (10) are

$$\begin{aligned} \hat{e}_i &= \dot{\hat{p}}_i - \hat{T} \dot{\bar{p}}_i - \tilde{\mathbf{T}} \dot{\bar{p}}_i \\ &= \dot{\hat{p}}_i - \text{Ad}_{\hat{T}} \left(\left[\tilde{b}_U - W_U \right]_{\wedge} \right) \tilde{\mathbf{T}} \bar{p}_i \end{aligned} \quad (28)$$

In the light of expressions in (2) and (3), one finds

$$\text{Ad}_{\hat{T}} \left([\tilde{b}_U - W_U]_{\wedge} \right) = \left[\overline{\text{Ad}}_{\hat{T}}(\tilde{b}_U - W_U) \right]_{\wedge} \text{ such that}$$

$$\text{Ad}_{\hat{T}}([\tilde{b}_U]_{\wedge}) \tilde{T} \bar{p}_i = \begin{bmatrix} [\hat{R}y_i + \hat{P}]_{\times} \\ \mathbf{I}_3 \end{bmatrix}^{\top} \overline{\text{Ad}}_{\hat{T}} \tilde{b}_U \quad (29)$$

Accordingly, the expression in (28) becomes

$$\dot{e}_i = \dot{\hat{p}}_i - \begin{bmatrix} [\hat{R}y_i + \hat{P}]_{\times} \\ \mathbf{I}_3 \end{bmatrix}^{\top} \overline{\text{Ad}}_{\hat{T}} (\tilde{b}_U - W_U) \quad (30)$$

Hence, the transformed error dynamics $\dot{E}_i = \Lambda_i(\dot{e}_i - \mu_i e_i)$ can be obtained by (21), given (10) and (30) for all $i = 1, 2, \dots, n$. Define the following candidate Lyapunov function $\mathcal{L} = \mathcal{L}(E_1, E_2, \dots, E_n, \tilde{b}_U)$

$$\mathcal{L} = \sum_{i=1}^n \frac{1}{2\alpha_i} \|E_i\|^2 + \frac{1}{2} \tilde{b}_U^{\top} \Gamma^{-1} \tilde{b}_U \quad (31)$$

From (21) and (31), and differentiating \mathcal{L} one obtains

$$\begin{aligned} \dot{\mathcal{L}} &= \sum_{i=1}^n \frac{1}{\alpha_i} E_i^{\top} \dot{E}_i - \tilde{b}_U^{\top} \Gamma^{-1} \dot{\tilde{b}}_U \\ &= - \sum_{i=1}^n \frac{1}{\alpha_i} E_i^{\top} \Lambda_i \begin{bmatrix} [\hat{R}y_i + \hat{P}]_{\times} \\ \mathbf{I}_3 \end{bmatrix}^{\top} \overline{\text{Ad}}_{\hat{T}} (\tilde{b}_U - W_U) \\ &\quad + \sum_{i=1}^n \frac{1}{\alpha_i} E_i^{\top} \Lambda_i (\dot{\hat{p}}_i - \mu_i e_i) - \tilde{b}_U^{\top} \Gamma^{-1} \dot{\tilde{b}}_U \end{aligned} \quad (32)$$

By (16) and (18) $|e_{i,k}| \leq \mu_{i,k} \bar{\delta}_{i,k} \xi_{i,k} |E_{i,k}|$, moreover, $\mu_{i,k}$ is a vanishing component. Consider $\bar{k}_{\delta} = \max\{\bar{\delta}_{1,1}, \bar{\delta}_{1,2}, \dots, \bar{\delta}_{n,3}\}$, $\bar{k}_{\xi} = \max\{\xi_{1,1}^0, \xi_{1,2}^0, \dots, \xi_{n,1}^0\}$, and the negative vanishing component $\bar{\mu} = \min\{\mu_{1,1}, \mu_{1,2}, \dots, \mu_{n,3}\} \leq 0$. Substituting W_U , $\dot{\tilde{b}}_U$ and $\dot{\hat{p}}_i$ with their definitions in (25), (24), and (23), respectively, one obtains

$$\begin{aligned} \dot{\mathcal{L}} &\leq -c_p \sum_{i=1}^n \frac{1}{\alpha_i} \|E_i\|^2 - k_w \left\| \sum_{i=1}^n \frac{1}{\alpha_i} \Lambda_i E_i \right\|^2 \\ &\quad - k_w \left\| \sum_{i=1}^n \frac{1}{\alpha_i} [\hat{R}y_i + \hat{P}]_{\times} \Lambda_i E_i \right\|^2 \end{aligned} \quad (33)$$

where $c_p = k_p - \bar{k}_{\delta} \bar{k}_{\xi} |\bar{\mu}|$ such that $k_p > \bar{k}_{\delta} \bar{k}_{\xi} |\bar{\mu}|$. Based on (33), $\dot{\mathcal{L}}$ is negative definite such that $\mathcal{L} \rightarrow 0$ which in turn implies that (E_1, E_2, \dots, E_n) converges asymptotically to \mathcal{S} defined in (26) for all $E_i(0) \in \mathcal{L}_{\infty}$ proving item (1) in Theorem 1. It becomes apparent that $\mathcal{L} \in \mathcal{L}_{\infty}$ and that a finite $\lim_{t \rightarrow \infty} \mathcal{L}$ exists. Given that $\bar{\delta}_{i,k} = \underline{\delta}_{i,k}$, and in the light of (16) and (18), it is given that

$$e_{i,k} = \bar{\delta}_{i,k} \xi_{i,k} \frac{\exp(E_{i,k}) - \exp(-E_{i,k})}{\exp(E_{i,k}) + \exp(-E_{i,k})}, \quad \bar{\delta}_{i,k} = \underline{\delta}_{i,k}$$

This implies that $E_{i,k} \neq 0$ for $e_{i,k} \neq 0$ and $E_{i,k} = 0$ only at $e_{i,k} = 0$ proving item (2) in Theorem 1. The fact that $E_{i,k}$ and $e_{i,k}$ converge to zero indicates that \ddot{E}_i and \ddot{e}_i remain bounded, and thereby \dot{E}_i and \dot{e}_i are uniformly continuous. Based on Barbalat Lemma, $\dot{E}_i \rightarrow 0$ and $\dot{e}_i \rightarrow 0$ as $t \rightarrow \infty$. According to the definition of \tilde{b}_U in (12) along with (24), $\dot{\tilde{b}}_U = -\dot{b}_U$, and as

a result $\dot{\tilde{b}}_U \rightarrow 0$ as $E_i \rightarrow 0$. Also, from (25), $W_U \rightarrow 0$ as $E_i \rightarrow 0$. Additionally from (23), $\dot{\hat{p}}_i \rightarrow 0$ as $E_i \rightarrow 0$ and $e_i \rightarrow 0$. Consequently, $\lim_{t \rightarrow \infty} \dot{\tilde{e}}_i = \lim_{t \rightarrow \infty} -\text{Ad}_{\hat{T}} \left([\tilde{b}_U]_{\wedge} \right) \tilde{T} \bar{p}_i = 0$ that is $\lim_{t \rightarrow \infty} \dot{\tilde{e}}_i = \lim_{t \rightarrow \infty} -\hat{T} [\tilde{b}_U]_{\wedge} \bar{y}_i = 0$. It follows that $\lim_{t \rightarrow \infty} [\tilde{b}_U]_{\wedge} \bar{y}_i = \lim_{t \rightarrow \infty} [-[y_i]_{\times}, \mathbf{I}_3] \tilde{b}_U = 0$ for all $i = 1, 2, \dots, n$. Let

$$M = \begin{bmatrix} -[y_1]_{\times} & \mathbf{I}_3 \\ \vdots & \vdots \\ -[y_n]_{\times} & \mathbf{I}_3 \end{bmatrix} \in \mathbb{R}^{3n \times 6}, \quad n \geq 3$$

As specified in Assumption 1, number of features is greater than or equal to 3. Thus M has full column rank and $\lim_{t \rightarrow \infty} M \tilde{b}_U = 0$ signifying that $\lim_{t \rightarrow \infty} \tilde{b}_U = 0$ showing item (3) in Theorem 1. Accordingly, from (33), $\dot{\mathcal{L}}$ is bounded. In the light of Barbalat Lemma, $\dot{\mathcal{L}}$ is uniformly continuous. Since both $\tilde{b}_U \rightarrow 0$ and $W_U \rightarrow 0$ as $t \rightarrow \infty$, $\hat{T} \rightarrow 0$ and in turn $\hat{T} \rightarrow T_c(R_c, P_c)$ where $T_c(R_c, P_c) \in \text{SE}(3)$ denotes a constant matrix with $R_c \in \text{SO}(3)$ and $P_c \in \mathbb{R}^3$. Thus, one concludes that $\lim_{t \rightarrow \infty} \hat{R} = R_c$ and $\lim_{t \rightarrow \infty} \hat{P} = P_c$ completing the proof. ■

V. SIMULATION RESULTS

This section explores the performance of the nonlinear observer for SLAM on the Lie group $\text{SLAM}_n(3)$ with systematic convergence. Consider the angular velocity to be $\Omega = [0, 0, 0.2]^{\top}$ (rad/sec) and the translational velocity to be $V = [1.8, 0, 0]^{\top}$ (m/sec). Let the true initial attitude and position of the vehicle be $R(0) = \mathbf{I}_3$ and $P(0) = [0, 0, 3]^{\top}$, respectively. Additionally, consider four features fixed with respect to the inertial-frame at the following locations: $p_1 = [8, 8, 0]^{\top}$, $p_2 = [-8, 8, 0]^{\top}$, $p_3 = [8, -8, 0]^{\top}$, and $p_4 = [-8, -8, 0]^{\top}$. In practice, b_U and n_U are non-zero. Hence, let the group velocity vector bias be $b_U = [b_{\Omega}^{\top}, b_V^{\top}]^{\top}$ with $b_{\Omega} = [0.09, 0.1, -0.1]^{\top}$ (rad/sec) and $b_V = [0.2, 0.2, -0.2]^{\top}$ (m/sec), and noise n_U of zero mean and standard deviation of 0.2. Let the initial estimate of attitude and position be $\hat{R}(0) = \mathbf{I}_3$ and $\hat{P}(0) = [0, 0, 0]^{\top}$, respectively, and let the initial estimates of the four features be $\hat{p}_1(0) = \hat{p}_2(0) = \hat{p}_3(0) = \hat{p}_4(0) = [0, 0, 0]^{\top}$. Design parameters and initial bias estimate are chosen as follows: $\alpha_i = 0.05$, $\Gamma = 10\mathbf{I}_6$, $k_w = 3$, $k_p = 3$, $\ell_{i,k} = 1$, $\xi_{i,k}^{\infty} = 0.1$, $\xi_{i,k}^0 = \bar{\delta}_{i,k} = \underline{\delta}_{i,k} = 1.2e_{i,k}(0) + 1.8$, and $\hat{b}_U(0) = \mathbf{0}_6$ for all $i = 1, 2, 3, 4$ and $k = 1, 2, 3$.

Fig. 3 depicts the true and estimated trajectories of the vehicle and the position of the features. The true vehicle trajectory is plotted as a solid black line with a black circle marking the final destination. The true feature positions are marked as black circles at p_1, p_2, p_3 and p_4 . Blue and red are used for the observer output. The estimated trajectory of the vehicle is represented by a blue dashed line which tracks the travel path from the origin (0,0,0) to its final destination marked with a blue star ★. The feature position estimates, indicated by the red dashed lines, initiate at the origin (0,0,0) and then gradually diverge to the true feature locations marked with red stars ★.

Both vehicle trajectory and feature positions commence at the origin with large initialization error and converge successfully to the true trajectory and locations, respectively. As such, Fig. 3 reveals impressive tracking capabilities of the proposed observer.

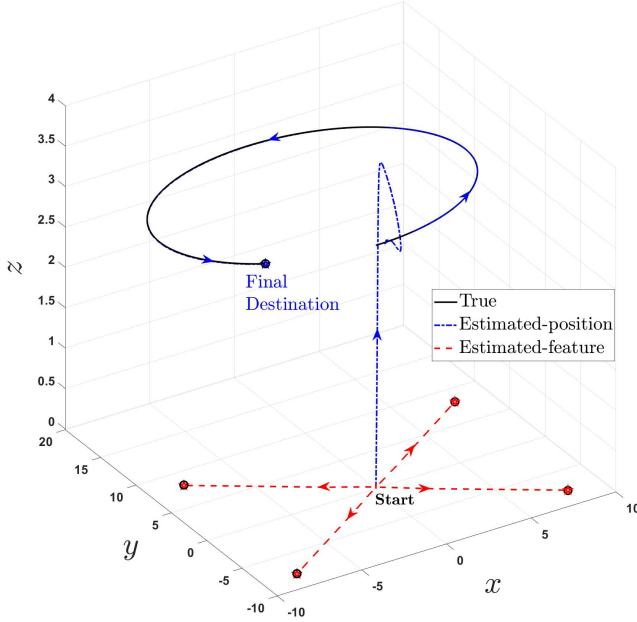


Fig. 3. Output trajectories of the observer vs true vehicle's and features position.

Fig. 4 illustrates the error trajectories of $e_i = [e_{i1}, e_{i2}, e_{i3}]^T$ for $i = 1, 2, 3, 4$ plotted in red, blue, and magenta with respect to the dynamically reducing boundaries of PPF plotted in black. As shown in Fig. 4 large initial error does not surpass the boundaries of the predefined large set and reduces following the dynamically reducing boundaries to a predefined small set. Therefore, the simulation results align with the theoretical results and demonstrate outstanding estimation capability of the proposed observer.

VI. CONCLUSION

This paper presented a novel nonlinear observer for Simultaneous Localization and Mapping (SLAM) problem on the Lie group of $\text{SLAM}_n(3)$. The observer has been developed such that the error function is guaranteed to follow predefined measures of transient and steady-state performance. Moreover, it is able to compensate for unknown bias attached to angular and translational velocities. As has been demonstrated in the Simulation Section, the proposed observer has the ability to produce reasonable results localizing the unknown pose of the vehicle and concurrently mapping the unknown environment with respect to available measurements of angular velocity, translational velocity, and features obtained in the body-frame.

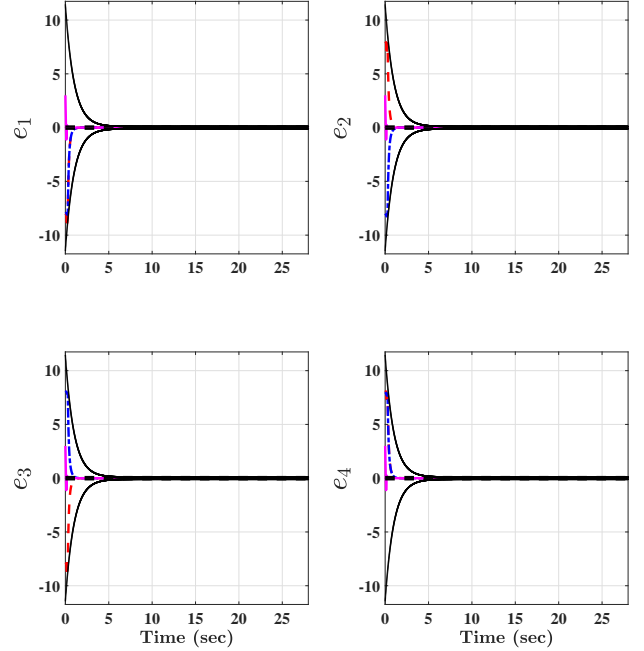


Fig. 4. Error trajectories of $e_i = [e_{i1}, e_{i2}, e_{i3}]^T$ for $i = 1, 2, 3, 4$ with respect to dynamically reducing boundaries of PPF.

ACKNOWLEDGMENT

The authors would like to thank **Maria Shaposhnikova** for proofreading the article.

REFERENCES

- [1] S. Thrun *et al.*, "Robotic mapping: A survey," *Exploring artificial intelligence in the new millennium*, vol. 1, no. 1-35, p. 1, 2002.
- [2] H. A. Hashim, L. J. Brown, and K. McIsaac, "Nonlinear pose filters on the special euclidean group SE(3) with guaranteed transient and steady-state performance," *IEEE Transactions on Systems, Man, and Cybernetics: Systems*, vol. PP, no. PP, pp. 1–14, 2019.
- [3] M.-D. Hua, T. Hamel, R. Mahony, and J. Trumpf, "Gradient-like observer design on the special euclidean group se(3) with system outputs on the real projective space," in *2015 54th IEEE Conference on Decision and Control (CDC)*. IEEE, 2015, pp. 2139–2145.
- [4] H. A. Hashim and F. L. Lewis, "Nonlinear stochastic estimators on the special euclidean group SE(3) using uncertain imu and vision measurements," *IEEE Transactions on Systems, Man, and Cybernetics: Systems*, vol. PP, no. PP, pp. 1–14, 2020.
- [5] H. A. Hashim, L. J. Brown, and K. McIsaac, "Nonlinear stochastic position and attitude filter on the special euclidean group 3," *Journal of the Franklin Institute*, vol. 356, no. 7, pp. 4144–4173, 2019.
- [6] M. Montemerlo and S. Thrun, *FastSLAM: A scalable method for the simultaneous localization and mapping problem in robotics*. Springer, 2007, vol. 27.
- [7] M. Kaess, A. Ranganathan, and F. Dellaert, "isam: Incremental smoothing and mapping," *IEEE Transactions on Robotics*, vol. 24, no. 6, pp. 1365–1378, 2008.
- [8] K. E. Bekris, M. Glick, and L. E. Kavraki, "Evaluation of algorithms for bearing-only slam," in *Proceedings 2006 IEEE International Conference on Robotics and Automation, 2006. ICRA 2006*. IEEE, 2006, pp. 1937–1943.
- [9] T. Zhang, K. Wu, J. Song, S. Huang, and G. Dissanayake, "Convergence and consistency analysis for a 3-d invariant-ekf slam," *IEEE Robotics and Automation Letters*, vol. 2, no. 2, pp. 733–740, 2017.

- [10] S. Huang and G. Dissanayake, "Convergence and consistency analysis for extended kalman filter based slam," *IEEE Transactions on robotics*, vol. 23, no. 5, pp. 1036–1049, 2007.
- [11] G. Grisetti, R. Kummerle, C. Stachniss, and W. Burgard, "A tutorial on graph-based slam," *IEEE Intelligent Transportation Systems Magazine*, vol. 2, no. 4, pp. 31–43, 2010.
- [12] C. Cadena, L. Carlone, H. Carrillo, Y. Latif, D. Scaramuzza, J. Neira, I. Reid, and J. J. Leonard, "Past, present, and future of simultaneous localization and mapping: Toward the robust-perception age," *IEEE Transactions on robotics*, vol. 32, no. 6, pp. 1309–1332, 2016.
- [13] H. Strasdat, "Local accuracy and global consistency for efficient visual slam," Ph.D. dissertation, Department of Computing, Imperial College London, 2012.
- [14] C. Forster, L. Carlone, F. Dellaert, and D. Scaramuzza, "On-manifold preintegration for real-time visual-inertial odometry," *IEEE Transactions on Robotics*, vol. 33, no. 1, pp. 1–21, 2016.
- [15] T. A. Johansen and E. Brekke, "Globally exponentially stable kalman filtering for slam with ahrs," in *2016 19th International Conference on Information Fusion (FUSION)*. IEEE, 2016, pp. 909–916.
- [16] R. Mahony and T. Hamel, "A geometric nonlinear observer for simultaneous localisation and mapping," in *2017 IEEE 56th Annual Conference on Decision and Control (CDC)*. IEEE, 2017, pp. 2408–2415.
- [17] D. E. Zlotnik and J. R. Forbes, "Gradient-based observer for simultaneous localization and mapping," *IEEE Transactions on Automatic Control*, vol. 63, no. 12, pp. 4338–4344, 2018.
- [18] C. P. Bechlioulis and G. A. Rovithakis, "Robust adaptive control of feedback linearizable mimo nonlinear systems with prescribed performance," *IEEE Transactions on Automatic Control*, vol. 53, no. 9, pp. 2090–2099, 2008.
- [19] H. A. Hashim, "Systematic convergence of nonlinear stochastic estimators on the special orthogonal group SO(3)," *International Journal of Robust and Nonlinear Control*, vol. 30, no. 10, pp. 3848–3870, 2020.
- [20] H. A. Hashim, L. J. Brown, and K. McIsaac, "Nonlinear stochastic attitude filters on the special orthogonal group 3: Ito and stratonovich," *IEEE Transactions on Systems, Man, and Cybernetics: Systems*, vol. 49, no. 9, pp. 1853–1865, 2019.
- [21] H. A. Hashim, "Special orthogonal group SO(3), euler angles, angle-axis, rodriguez vector and unit-quaternion: Overview, mapping and challenges," *arXiv preprint arXiv:1909.06669*, 2019.

where $\mathbf{Y}(\hat{Q}, y_i) \in \mathbb{R}^3$, $x \in \mathbb{R}^3$ and $\hat{Q} \in \mathbb{S}^3$. The equivalent quaternion representation and complete implementation steps of the observer in (22), (23), (24), and (25) is:

$$\left\{ \begin{array}{l} \overset{\circ}{e}_i = \bar{p}_i - \hat{T} \bar{y}_i = [e_i^\top, 0]^\top, \quad i = 1, 2, \dots, n \\ E_{i,k} = \frac{1}{2} \ln \frac{\delta_{i,k} + e_{i,k}/\xi_{i,k}}{\delta_{i,k} - e_{i,k}/\xi_{i,k}}, \quad k = 1, 2, 3 \\ \overline{\text{Ad}}_{\hat{T}}^\top = \begin{bmatrix} \mathcal{R}_{\hat{Q}}^\top & -\mathcal{R}_{\hat{Q}}^\top [\hat{P}]_\times \\ 0_{3 \times 3} & \mathcal{R}_{\hat{Q}}^\top \end{bmatrix} \\ \overline{\text{Ad}}_{\hat{T}^{-1}} = \begin{bmatrix} \mathcal{R}_{\hat{Q}}^\top & 0_{3 \times 3} \\ -\mathcal{R}_{\hat{Q}}^\top [\hat{P}]_\times & \mathcal{R}_{\hat{Q}}^\top \end{bmatrix} \\ \chi = \Omega_m - \hat{b}_\Omega - W_\Omega \\ \dot{\hat{Q}} = \frac{1}{2} \begin{bmatrix} 0 & -\chi^\top \\ \chi & -[\chi]_\times \end{bmatrix} \hat{Q}, \quad \hat{Q}(0) = Q_I \\ \dot{\hat{P}} = \mathbf{Y}(\hat{Q}, V_m - \hat{b}_V - W_V) \\ \dot{\hat{p}}_i = -k_p (\Lambda_i + \Lambda_i^{-1}) E_i \\ \dot{\hat{b}}_U = -\sum_{i=1}^n \frac{\Gamma}{\alpha_i} \overline{\text{Ad}}_{\hat{T}}^\top \begin{bmatrix} [\mathbf{Y}(\hat{Q}, y_i) + \hat{P}]_\times \\ \mathbf{I}_3 \end{bmatrix} \Lambda_i E_i \\ W_U = -\sum_{i=1}^n k_w \overline{\text{Ad}}_{\hat{T}^{-1}} \begin{bmatrix} [\mathbf{Y}(\hat{Q}, y_i) + \hat{P}]_\times \\ \mathbf{I}_3 \end{bmatrix} \Lambda_i E_i \end{array} \right.$$

APPENDIX

Quaternion Representation

Define $Q = [q_0, q^\top]^\top \in \mathbb{S}^3$ as a unit-quaternion with $q_0 \in \mathbb{R}$ and $q \in \mathbb{R}^3$ such that $\mathbb{S}^3 = \{Q \in \mathbb{R}^4 \mid \|Q\| = \sqrt{q_0^2 + q^\top q} = 1\}$. $Q^{-1} = [q_0 \quad -q^\top]^\top \in \mathbb{S}^3$ denotes the inverse of Q . Define \odot as a quaternion product where the quaternion multiplication of $Q_1 = [q_{01} \quad q_1^\top]^\top \in \mathbb{S}^3$ and $Q_2 = [q_{02} \quad q_2^\top]^\top \in \mathbb{S}^3$ is

$$Q_1 \odot Q_2 = \begin{bmatrix} q_{01}q_{02} - q_1^\top q_2 \\ q_{01}q_2 + q_{02}q_1 + [q_1]_\times q_2 \end{bmatrix}$$

The mapping from unit-quaternion (\mathbb{S}^3) to $\mathbb{S}\mathbb{O}(3)$ is described by $\mathcal{R}_Q : \mathbb{S}^3 \rightarrow \mathbb{S}\mathbb{O}(3)$

$$\mathcal{R}_Q = (q_0^2 - \|q\|^2)\mathbf{I}_3 + 2qq^\top + 2q_0 [q]_\times \in \mathbb{S}\mathbb{O}(3) \quad (34)$$

The quaternion identity is described by $Q_I = [\pm 1, 0, 0, 0]^\top$ with $\mathcal{R}_{Q_I} = \mathbf{I}_3$. Visit [21] for more information. Define the estimate of $Q = [q_0, q^\top]^\top \in \mathbb{S}^3$ as $\hat{Q} = [\hat{q}_0, \hat{q}^\top]^\top \in \mathbb{S}^3$ with

$$\mathcal{R}_{\hat{Q}} = (\hat{q}_0^2 - \|\hat{q}\|^2)\mathbf{I}_3 + 2\hat{q}\hat{q}^\top + 2\hat{q}_0 [\hat{q}]_\times \in \mathbb{S}\mathbb{O}(3)$$

see the map in (34). Define the map

$$\begin{bmatrix} 0 \\ \mathbf{Y}(\hat{Q}, x) \end{bmatrix} = \hat{Q} \odot \begin{bmatrix} 0 \\ x \end{bmatrix} \odot \hat{Q}^{-1}$$